Journal on Surgery

www.journalonsurgery.org

Research Article

Open Access, Volume 2

Homologous Recombination Deficiency and ERBB2 Alterations as Differential Diagnosis and Personalized Treatment Options in Primary Pulmonary Enteric Adenocarcinoma

Zhong L; Zhang CF; Jia WT; Zhang PX*

Departments of Pathology, First Affiliated Hospital of Dalian Medical University, Dalian, China.

Abstract

Background: Primary Pulmonary Enteric Adenocarcinoma (PEAC) is a special and rare subtype of lung adenocarcinoma. There is very little data on differential diagnosis from Metastasis Colonrectal Cancer (MCC) and potentially treatable molecular alterations in PEAC.

Methods: We retrospectively evaluated immunostaining profile and the classic driven genes signatures in 6 PEACs and 16 MCCs, using immunohistochemistry and real-time PCR. Additionally, mismatch repair deficiency and Homologous Recombination Deficiency (HRD) were analyzed by sequencing.

Results: The study revealed the immunohistochemical profile based on CK7 and Villin positivity of PAEDs appears robust to support this diagnosis. ERBB2 amplication was detected in one of 3 HER2 immunopositivity cases in PEACs. Molecular analysis revealed KRAS as the most frequently mutated gene in PEACs (33.3%) and MCCs (37.5%), but the carried ERBB2 mutation for PEAC is unique to MCC. No high Microsatellite Instability (MSI-H) and PD-L1 stainning were detected in PEACs. The potential deficiency in homologous recombination pathway was found in 50% of PEACs and 87.5% of MCCs. PEACs had the higher HRD score than MCCs, but only one PEAC case was identified the high HRD score (≥42).

Conclusion: Our investigation showed a classification model by immunohistochemical marker, intergrading genetic signature of ERBB2 mutation / amplication and HRD, to accurately diagnose PEAC. Furthermore, our results underscore the relevance of potentially treatable molecular alterations in PEAC, like ERBB2 and HRD. Evaluation of HRD score may help select patients that could benefit from platinum-based chemotherapy and PARP inhibitors treatments in PEAC.

Keywords: ERBB2 gene; Homologous recombination deficiency; PARP inhibitors; PD-L1 expression; Primary pulmonary enteric adenocarcinoma.

Manuscript Information: *Received: Mar 20, 2022; Accepted: Apr 11, 2022; Published: Apr 14, 2022*

Correspondance: *Pengxin Zhang, Departments of Pathology, First Affiliated Hospital of Dalian Medical University, No. 222, Zhongshan Road, Xigang District, Dalian City, Liaoning Province, 116001, The People's Republic of China.*

Tel: +86-18098877181, Fax: +86-041183622844; Email: Zhangpengxin1983@163.com

Citation: *Zhong L, Zhang CF, Jia WT, Zhang PX. Homologous Recombination Deficiency and ERBB2 Alterations as Differential Diagnosis and Personalized Treatment Options in Primary Pulmonary Enteric Adenocarcinoma. J Surgery. 2022; 2(1): 1017.*

Introduction

During the past several decades, lung cancer has been the leading cause of cancer death. Pulmonary adenocarcinoma has displaced squamous cell carcinoma as the most common form of Non-Small Cell Lung Cancer (NSCLC). Pulmonary adenocarcinoma is morphologically heterogeneous, representing a wide variety of histological patterns. A new lung adenocarcinoma classification based on predominant histological patterns was proposed by the International Association for the Study of Lung Cancer (IASLC), American Thoracic Society (ATS), and European Respiratory Society (ERS) in 2011 [1]. Primary Pulmonary Enteric Adenocarcinoma (PEAC) was a rare subtype of lung adenocarcinoma, which was first described by Tsao and Fraser in 1991 [2]. It was defined as an entero-like morphology in more than 50% of tumor cells, and expression of least one major immunohistochemical markers of intestinal differentiation, namely Cytokeratin 20 (CK20), Caudal Type Homeobox (CDX2) and/or Mucin 2 (MUC2) [3]. The positive staining for Cytokeratin 7 (CK7), Thyroid Transcription Factor-1 (TTF-1) and/or NapsinA in approximately 50% of cases also favored the PEAC diagnosis [3,4]. Molecular analysis revealed KRAS was the most frequently mutated gene (>60% of cases), and very few cases harbored abnormalities affecting EGFR, ALK, ROS1, NRAS, BRAF and ERBB2 genes in PEAC [5-9].

Programmed Death Ligand-1 (PD-L1) and Programmed Death-1 (PD-1) expression have been shown to be associated with a response to immunotherapy in a number of malignancies. PD-1 blockade provided a therapeutic opportunity for patients with high Tumor Mutation Burden (TMB), High Microsatellite Instability (MSI-H), Deficient Mismatch Repair (dMMR) and/or positive Programmed Cell Death Ligand-1 (PD-L1) expression [10-12]. Defects in mismatch repair is Microsatellite Instability (MSI), five biomarkers that contain monoucleotide or dinucleotide repeats in specific regions of the genome are used for clinical determination of MSI status [13]. Immunohistochemistry using antibodies against MLH1, MSH2, MSH6 and PMS2 is another effective technique to assess MMR status [11,13]. Several subsequent studies confirmed the presence of somatic MMR genes mutations in PAED lesions [6,7,14]. Recently, the potential target for treatment with immune checkpoint inhibitors in PAED patients were confirmed, according to the validated presence of a high TMB but also of the membranous PD-L1 staining positivity in the tumor cells of PAED [15].

Genetic defects, including mismatch repair and homologous recombination pathways, might confer repair-deficient characteristics. In the context of distinct cancers types, such as breast and ovarian, genome instability is typically attributed to defects in homologous recombination DNA repair genes, not the defects of mismatch repair pathway [16,17]. Homologous Recombination Deficiency (HRD) can occur in cells with detectable BRCA1/2 mutations or exhibiting BRCA-ness phenotypes [18]. The inhibitors of Poly (ADP)-Ribose Polymerase (PARPi) are effectively used to treat cancers that carry mutations in BRCA1/2 or BRCA-ness phenotypes. The choice of PARP inhibitor is mainly based upon the presence of defects in BRCA1/2 and other HR pathway genes [19]. The measurement of Homologous Recombination Deficiency (HRD) in cancer is therefore vital to the target therapy incorporating PARP inhibitors. Recently, three SNP array-based signatures of chromosomal instability that each quantitated a distinct type of genomic scars considered to be caused by improper DNA repair, namely loss of heterozygosity profiles (Homologous Recombination Deficiency-Loss of Heterozygosity (HRD-LOH) score), telomeric allelic imbalance (Homologous Recombination Deficiency- Telomeric Allelic Imbalance (HRD-TAI) score), and large-scale state transitions (Homologous Recombination Deficiency-Large-Scale State Transition (HRD-LST) score) were published [20-22]. All three scores were highly correlated with defects in BRCA1/2 and other HR pathway genes in breast cancer or ovarian cancer, and were associated with sensitivity to platinum agents [20-22].

Advances in the molecular characteristics of PAED will certainly improve its differential diagnosis and personalized therapy. The status of DNA homologous recombination repair genes are still not thoroughly investigated in PEAD. Here, we investigated alterations of DNA repair genes, using next generation sequencing based assay that could be used to calculate all three genomic scare scores to examine HRD. It could provide a new method to differential diagnosis from Metastasis Colonrectal Cancer (MCC) and expand the spectrum of personalized therapy options for PEAD.

Methods

Patients and tissue specimens

We retrospectively collected data from 6 PEAC patients and 16 MCC patients for this study. The specimens were obtained from patients who underwent complete surgical resection from 2012 to 2020 at the First Affiliated Hospital of Dalian Medical University. The clinicopathological factors of the patients are shown in **Table 1**. All of the procedures were approved by the Ethics Committee on Human Research of the First Affiliated Hospital of Dalian Medical University, and written informed consent was obtained from all of the patients before surgery.

Immunohistochemistry analysis

Serial tissue sections of 4μm thickness sliced from paraffin-embedded specimens were used for immunohistochemistry using the labeled streptavidin-biotin method. The antibodies are listed in Table S1. The slides were deparaffinized with xylene and rehydrated with ethanol. Then, antigen retrieval via EDTA (pH 9.0) was carried out by autoclaving the slides. Immunohistochemical staining was performed on the Dako Autostainer Link 48 (PD-L1) and Roche Ventana BenchMark XT (TTF-1, CK7, NapsinA, CK20, Villin, CDX2, MUC2, Ki-67, P53, ERBB2 (c-erbB-2 or HER2), MLH1, MSH2, MSH6, PMS2, PD-1) automated slide stainer according to the instructions supplied by manufacturer. The scoring method for ERBB2 expression was based on the cell membrane staining. 3+, uniformintense complete membrane strong staining of more than 10% of invasive tumor cells; 2+, nonuniformer complete membrane weak staining > 10% or uniformintense complete membrane strong staining <10% of invasive tumor cells; 1+, incomplete membrane weak staining in at least 10% of cells; 0+, negative for ERBB2 protein expression [23]. PD-L1 staining was considered positive if the tumor cell membrane was partially or completely stained >1%, irrespective of the staining intensity [24]. All available tumor slides were reviewed by two pathologists, using an Olympus BX51 microscope (Olympus, Tokyo, Japan) with a standard 22-mm diameter eyepiece.

Fluorescence in situ hybridization (FISH)

The assay was performed on unstained 5μm thickness sections from paraffin-embedded specimens, according to manufacturers' test kit protocols (PathVysion Kit, USA). Scoring was performed by two pathologists. Two-color FISH analysis was performed by counting chromosome 17 centromere signals (CEP17; green) and ERBB2 gene-specific signals (red) within 20 nuclei of invasive cancer cells and then calculating the ratio of Red: Green signals. Positive ERBB2 amplification: FISH ratio≥ 2 or ratio < 2. and but the average ERBB2 signal number ≥ 6.0 or ERBB2 signals are connected as cluster; Equivocal ERBB2 amplification: FISH ratio < 2.0 and the average ERBB2 signals number between 4.0 ~ 6.0, the specimen was undetermined, that require to count additional 20 cells and recalculate to interpret the result; Negative ERBB2 amplification: FISH ratio < 2.0 and the average ERBB2 signals number < 4.0 [25].

Gene mutation analysis

All patients in our study were routinely examined for molecular aberrations at diagnosis. The mutation genes are listed in Table S2. Genomic DNA was extracted from paraffin-embedded specimens using a QIAamp DNA FFPE tissue kit (QIAGEN, Hilden, Germany), subsequently diluted to 2ng/μL. DNA quantification was performed using the Qubit 2.0 fluorimeter with the dsDNA HS assay kits (Life Technologies, Carlsbad, CA). The mutations were analyzed using the Amplification Refractory Mutation System (ARMS) by commercially available ADx mutation detection kits (AmoyDx, Ltd., Xiamen, China), followed by an fluorescent quantitative PCR instrument of ABI 7500 (Applied Biosystems; Thermo Fisher Scientific Inc., USA). The results were interpreted according to manufacturer's protocals.

Analysis of microsatellite instability

MSI analysis was performed using the commercially available ADx MSI analysis kits (AmoyDx, Ltd., Xiamen, China) with the following 5 microsatellite markers: BAT-26, CAT-25, BAT-25, MONO-27 NR-24 and paired non-tumorous lung tissues DNA (>5cm far from the tumorous tissues) of the same case. Genomic DNA was extracted from paraffin-embedded specimens using a QIAamp DNA FFPE tissue kit (QIAGEN, Hilden, Germany). PCR was performed using DNA at 5ng/μl. PCR products were then submitted to capillary electrophoresis on an ABI 3500XL genetic analyzer (Applied Biosystems, Foster City, USA) according to the manufacturer's instructions. The results were analyzed using GeneMapper v4.1 (Applied Biosystems, Foster City, USA) software to measure the fragment length in base pairs. A fragment of peak exceeded the control width> 3 base pairs were defined as MSI. We classified the tumors as High-Frequency MSI (MSI-H) if two or more of the five markers showed MSI and Low-Frequency MSI (MSI-L) if any one marker showed MSI. Microsatellite Stable (MSS) was characterized by the absence of MSI by all 5 markers [13].

Next Generation Sequencing (NGS)

Next generation sequencing was performed in FFPE-isolated tumor with a 54 genes panel including 34 genes involved in the Homologous Recombination Repair (HRR) pathway, six Mismatch Repair (MMR) genes, four Base Excision Repair (BER) genes and ten other related genes, using the commercially available ADx HRD analysis kits (AmoyDx, Ltd., Xiamen, China) (Table S3). The libraries were prepared using SureSelectQXT library prep kit (Agilent) according to manufacturer's instructions and sequenced on Nextseq 500/Miseq (Illumina, San Diego, CA). Library amplification was performed using Herculase II fusion DNA polymerase (Agilent) and the PCR product was purified using the Agencourt AMPureXP purification bead system (Beckman Coulter; Pasadena, CA). The analysis of amplified indexed library DNA was performed using high sensitivity D1000 ScreenTape (on Agilent TapeStation). Two samples were excluded (DNA quantity and quality) and 31 were multiplexed into 1.4 pM pool and loaded onto the Nextseq 500/Miseq. Pathogenic mutations were determined by a clinical molecular geneticist according to the guidelines of American College of Medical Genetics (ACMG) [25].

Homologous recombination deficiency scores

Details of the individual LOH, TAI and LST scores, as well as the combined HRD score, were calculated as Marquard et al. described [26]. In summary, LST indicated the number of chromosomal breaks between adjacent regions of at least 10Mb (high: >15 in diploid tumors and >20 in polyploidy tumors); TAI was referred as the number of subtelomeric regions with allelic imbalance that started beyond the centromere and extended to the telomere region (high: > median value). LOH indicated the number of LOH regions larger than 15Mb and shorter than the whole chromosome (high: >10). HRD status was determined on the basis of the combination of the dichotomized HRD scores using the predefined HRD threshold and tumor BRCA1/2 status (scored as mutated if deleterious or suspected deleterious mutations in BRCA1/2 were present; nonmutated if otherwise, including variants of uncertain significance). HR deficiency was defined as high HRD score (above the HRD threshold, ≥42) and/or mutated tumor BRCA1/2. HR nondeficiency was defined as low HRD score (below the HRD threshold, <42) and nonmutated or failed tumor BRCA1/2 mutation analysis.

Statistical analysis

Statistical analyses were performed using IBM SPSS statistics 22.0 (IBM Co., Armonk, NY, USA). Pearson's $\chi 2$ test or Fisher's exact test was used to assess the association between two categorical variables. Independent sample t-test was applied to investigate correlation between two continuous variables. Some figures were generated using the R package ggplot2 and RColorBrewer. P-values were two-tailed for all the tests. Statistical significance $P < 0.05$ was deemed to indicate statistical significance.

Results

Clinicopathological characteristics of patients

A total of 6 PEAC and 16 MCC patients were identified. The clinicopathological data is summarized in Table 1. A comparison of clinicopathological data for the PEAC and MCC groups revealed no statistically significant in terms of age, sex, smoking status, lymph node metastases, site of the main tumor, location type (central or peripheral), and serum tumor markers (CEA and CA199). Compared with MCCs, patients with PEAC had larger lesions (P=0.044) with a more early pathological stage (P<0.001). Pleural invasion was more frequently found in PEACs than MCCs (P=0.025). Of all 22 patients, 5 PEAC and 4 MCC patients survived and 13 patients were died to follow-up ending on December 31, 2020 (3-32 months). The median survival of PEACs were longer

than MCCs (P=0.021).

Immunohistochemistry results in PEACs and MCCs

Detailed immunohistochemical characteristics are shown in Table 2. The pneumocyte markers (CK7, TTF-1, NapsinA) and the enteric markers (Villin, CK20, CDX-2, MUC2) were tested in PEACs and MCCs. Positive staining for CK7 was also positive for Villin in all 6 PEAC patients, whereas the expressions of NapsinA and MUC2 were negative (Table 2, Figure 1A). Positive TTF-1, CK20 and CDX-2 expressions were detected in 2/6 (33.33%), 3/6 (50.00%) and 2/6 (33.33%) patients of PEAC, respectively. The expressions of CK7 and NapsinA were found to be negative in all 16 MCCs, of which 2 patients were positive for TTF-1. However, the expressions of Villin, CK20 and CDX-2 were positive in all MCCs (Table 2, Figure 1A). It was found that expression of CK7 and Villin could aid in the differential diagnosis of PEAC. Of note, compared to P53 immunopositivity (33.3%) for PEACs, MCCs showed a higher positive rates on P53 with 87.5% (**Table 2**, P=0.025). For comparison, the mean Ki-67 proliferation index for PEACs was 48.33%, MCCs showed higher proliferation rates in Ki-67 IHC with a mean of 75.94% (Figure 1A and Table 2, P<0.001).

Furthermore, a total of 3 out of 6 (50%) PEACs were positive for ERBB2 (Figure 1B), but ERBB2 expressions were negative in all 16 MCCs. ERBB2 immunopositivity had significant difference between PEACs and MCCs (Table2, P=0.013). It could be observed that ERBB2 was a more valuable molecular marker for the differential diagnosis in PEAC from MCC. An additional analysis was performed to assess for ERBB2 gene copy number alterations by FISH. Amplification of ERBB2 was detected in only one cases of 3 positive ERBB2 expression for the PEAC patients (Figure 1B).

Gene mutation characteristics in PEACs and MCCs

The mutation analysis results are illustrated in Table 3 and Table S4. All patients in our study were routinely examined for molecular aberrations, including classic driver genes for NSCLC (EGFR, ALK, ROS1, RET, ERBB2, Met exon14 skipping) and for colorectal carcinoma (KRAS, NRAS, BRAF, PIK3CA) by ADx-ARMS Polymerase Chain Reaction (PCR). In PEAC patients, KRAS mutations were present as the most commonly mutated gene (2/6, 33.3%, Table 3), whereas no mutations in EGFR, ALK and ROS1 were detected. Although PAED samples did not harbor EGFR mutations in exons 18-21, which were the most frequently detected in 30% of lung adenocarcinomas, whereas ERBB2 mutations were found only in one sample (1/6, 16.7%, Table 3). In MCC patients, the typical KRAS mutations were identified in six out of 16 MCC samples (37.5%), while NRAS and PIK3CA mutations occurred in one cases (1/16, 6.25%, Table 3). None of the other specific mutations were detected in MCCs. The mutation frequencies were relatively similar for KRAS in PEACs and MCCs (33.3 versus 37.5%, **Table 3**, P=0.856). The carried ERBB2 mutation for PEAC was unique to MCC (Table 3, P=0.095), confirming the different pathogenesis to MCC.

Immune checkpoint blockade MSI and PD-L1 distributions in PEACs and MCCs

The high percentage of KRAS mutations resulted in an intrinsic resistance of these tumors to tyrosine kinase inhibitors, which suggested a potential eligibility for treatment with immune checkpoint inhibitors. Expression analysis of MMR proteins (MLH1, PMS2, MSH2 and MSH6) was performed. All the 6 PEACs presented expression of the four MMR proteins, thus being considered positive (Figure 2A). Among 16 MCCs, only one case (1/16, 6.25%) displayed combined loss of MLH1 and PMS2 expression, thus being considered negative, which was subsequently analyzed for MSI and confirmed to be negative (Table 2, Figure 2A).We observed that all the 6 PEADs and 15 MCCs were MSS, only one MCC case was MSI-H, which had the following four common instability markers: BAT-26, BAT-25, CAT-25 and MONO-27 (Table 3, Figure 2B). Of interest, there were no expression of PD-1 and PD-L1 in tumor cells membrane compartment in all the PEADs and MCCs, while PD-1 staining was positive in interstitial immune cells of some cases (Figure 2C). In addition, the expression of PD1 and PD-L1 in the only one MSI-H case was also negative in tumor cells.

Homologous recombination deficiency in PEACs and MCCs

HRD is an important clinical correlation in strongly predicting response to platinum-based therapies and PARP inhibition. We investigated somatic mutations in harboring 54 HRD-related genes panel, including BRCA1 and BRCA2. Results of the mutation screening analysis are shown in Table S5. TP53 was the gene with the highest mutation rate (68.2%, 15/22), followed by FANCA, ATR and MRE11 (Figure 3A). Potential deficiency in HR pathway (at least one HRD related gene) was found in 50% of PEACs and 87.5% of MCCs (Table S5). Three PEAC cases presented HR genes mutation, including CHEK1, FANCA, KMT2D, STK11, WRN (Figure 3A). Fourteen MCC cases presented HR genes mutation, including ATM, ATRX, FANCA, FANCC, FANCI, MRE11, PALB2, RAD51B and WRN (Figure 3A). Three cases harbored MMR gene mutations, MSH6 (PEAC6) and PMS2 (PEAC1, MCC9), but all MMR gene mutations in PEACs were intronic mutations (Figure 3A).

HRD scores are considered biomarkers of genomic instability and analyzed in our patients. HRD status positive (HRD score ≥ 42 or BRCA1/2 mutant) or negative (HRD score < 42 and BRCA1/2 wild type) was concordant for all patients. BRCA1 and BRCA2 alterations had the largest weight for predicting HRD status positive, but we detected no somatic deleterious mutations of BRCA1 and BRCA2 in 6 PAED and 16 MCC patients (Figure 3A, Table S5). The HRD score on median values of TAI, LST and LOH were higher in PEACs than MCCs, respectively (Figure 3B, Table 4). LOH score was the lowest score in PEACs and MCCs. PEACs had the higher combined scores than MCCs (Figure 3B, Table 4, P<0.001). Using HRD scores ≥ 42 as cut-off for high scores, only one PEAC case with a profile enough to be classified as HRD-high was found in all 6 PEACs and 16 MCCs (Table S6, case PEAC5, score N=51). This HRD-high case had a co-existing MSH6 mutation but no mutations in other HRD-related gene. The significant difference of the HRD score levels was found between the PEACs and MCCs, indicating that the elevation of HRD levels might be PEAC specific.

Table 1: Clinicopathological characteristics of PEACs in comparison with MCC.

Clinical factors	PEAC		MCC		P-value
	N	%	N	%	
Age, mean±SD (y) [a]	62.00 ± 6.87 (53-71)		65.06 ± 7.76 (54-80)		0.407
Sex [b]					
Female	4	66.7	8	50	0.646
Male	2	33.3	8	50	
Smoking history [b]					
Never	5	83.3	10	62.5	0.616
Former/current	1	16.7	6	37.5	
Size, mean±SD (cm) [a]	3.98 ± 2.00 (1.3-6)		2.24 ± 1.57 (1-6)		0.044
Pathological stage [c]					
I	1	16.7	0	0	<0.001
II	4	66.6	0	0	
III	1	16.7	0	0	
IV	0	0	16	100	
Lymph node metastases [b]					
N0	5	88.3	15	93.75	0.481
N1/N2	1	16.7	1	6.25	
Pleural invasion [b]					
Yes	4	66.7	2	12.5	0.025
No	2	33.3	14	87.5	
Site of the main tumor [c]					
LUL	2	33.3	5	31.25	0.342
LLL	2	33.3	1	6.25	
RUL	0		2	12.5	
RML	1	16.7	1	6.25	
RLL	1	16.7	7	43.75	
Location type [b]					
Central	1	16.7	1	6.25	0.481
Peripheral	5	88.3	15	93.75	
Serum tumor Markers[a]					
CEA, ng/mL	2.12 ± 1.26		4.03 ± 3.79		0.246
CA19-9, U/mL	9.99 ± 7.84		12.97 ± 21.20		0.743
Follow-up mean±SD(Month) [a]					
Died	18		9.67 ± 5.48		0.172
Alive	22 ± 8.28		8.75 ± 3.40		0.021

PEAC: Pulmonary Enteric Adenocarcinoma; MCC: Metastasis Colonrectal Cancer; LLL: Left Lower Lobe; LUL: Left Upper Lobe; RLL: Right Lower Lobe; RML: Right Middle Lobe; RUL: Right Upper Lobe; SD: Standard Deviation; CA19-9: Carbohydrate Antigen 19-9; CEA: Carcinoembryonic Antigen; the normal expression ranges of these four tumor markers: CEA, 0-5 µg/L; CA199, 0-37 U/mL. [a]Student t-test, [b]Fisher's exact test, [c]Pearson Chi-Square test for the differences between PEACs and MCCs.

Table 2: Immunohistochemistry results of PEACs and MCCs.

	PEAC(N=6)		MCC(N=16)		
Makers	**Positive (%)**	**Negative (%)**	**Positive (%)**	**Negative (%)**	**P-value**
CK7	6/6(100)	0/6(0)	0/16(0)	16/16(100)	<0.001
TTF-1	2/6(33.3)	4/6(66.7)	2/16(12.5)	14/16(87.5)	0.292
NapsinA	0/6(0)	6/6(100)	0/16(0)	16/16(100)	<0.001
CK20	3/6(50)	3/6(50)	16/16(100)	0/16(0)	0.013
Villin	6/6(100)	0/6(0)	16/16(100)	0/16(0)	0.037
CDX2	2/6(33.3)	4/6(66.7)	16/16(100)	0/16(0)	0.002
MUC2	0/6(0)	6/6(100)	10/16(62.5)	6/16(37.5)	0.015
ERBB2	3/6(50)	3/6(50)	0/16(0)	16/16(100)	0.013
Ki-67, mean±SD	48.33% ± 7.53%		75.94% ± 15.19%		<0.001
P53	2/6(33.3)	4/6(66.7)	14/16(87.5)	2/16(12.5)	0.025
MLH1	6/6(100)	0/6(0)	15/16(93.75)	1/16(6.25)	1.000
MSH2	6/6(100)	0/6(0)	16/16(100)	0/16(0)	-
MSH6	6/6(100)	0/6(0)	16/16(100)	0/16(0)	-
PMS2	6/6(100)	0/6(0)	15/16(93.75)	1/16(6.25)	0.531
PD-1	2/6(33.3)	4/6(66.7)	3/16(18.75)	13/16(81.25)	0.585
PD-L1	0/6(0)	6/6(100)	0/16(0)	16/16(100)	

CK: Cytokeratin; TTF-1: Thyroid Transcription; Napsin A: Ovel Aspartic Proteinase of the Pepsin Family A; CDX-2: Caudal Type Homeobox Transcription Factor 2; MUC2: Mucin-; MLH1: Mutl Homolog 1; MSH2: Muts Homolog 2; MSH6: Muts Homolog 6; PMS2, PMS1 Homolog 2; Mismatch Repair System Component; PD-1: Programmed Death-1; PD-L1: Programmed Death-Ligand 1.

Table 3: Molecular markers of PEACs and MCCs.

Makers	PEAC(N=6)		MCC(N=16)		P-value
	Mutated/ Fusion (%)	**Wild type (%)**	**Mutated/ Fusion (%)**	**Wild type (%)**	
EGFR	0/6(0)	6/6(100)	0/16(0)	16/16(100)	-
KRAS	2/6(33.3)	4/6(66.7)	6/16(37.5)	10/16(62.5)	0.856
NRAS	0/6(0)	6/6(100)	1/16(6.25)	15/16(93.75)	0.531
BRAF	0/6(0)	6/6(100)	0/16(0)	16/16(100)	-
PIK3CA	0/6(0)	6/6(100)	1/16(6.25)	15/16(93.75)	0.531
ERBB2	1/6(16.7)	5/6(83.3)	0/16(0)	16/16(100)	0.095
MET	0/6(0)	6/6(100)	0/16(0)	16/16(100)	-
ALK	0/6(0)	6/6(100)	0/16(0)	16/16(100)	-
ROS1	0/6(0)	6/6(100)	0/16(0)	16/16(100)	-
RET	0/6(0)	6/6(100)	0/16(0)	16/16(100)	-
MSI	0/6(0)	6/6(100)	1/16(6.25)	15/16(93.75)	0.531

EGFR: Epidermal Growth Factor Receptor; KRAS: Kirsten Rat Sarcoma Viral Oncogene; BRAF: V-Raf Murine Sarcoma Viral Oncogene Homolog B1; NRAS: N-Formyl-L-Kynurenine Neuroblastoma Rat Sarcoma Viral Oncogene Homolog; PIK3CA: Phosphatidylinositol-4,5-Bisphosphate 3-Kinase Catalytic Subunit Alpha; ERBB2: Avian Erythroblastic Leukemia Viral Oncogene Homolog 2; MET: Mesenchymal To Epithelial Transition Factor; ALK: Anaplastic Lymphoma Kinase; ROS1: Receptor Tyrosine Kinase C-Ros Oncogene 1; RET: Proto-Oncogene C-Ret; MSI: Microsatellite Instability.

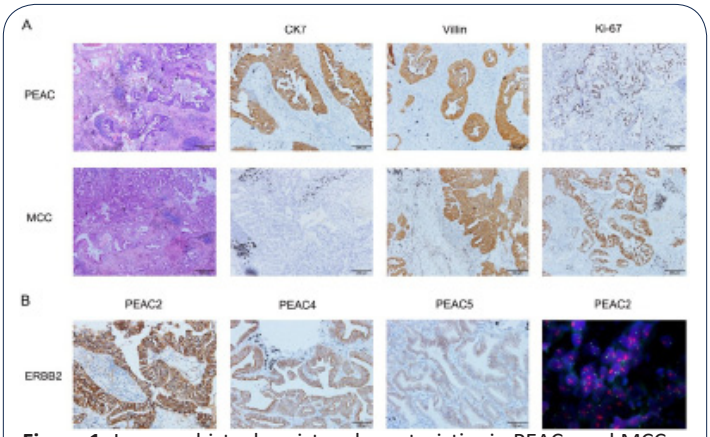

Figure 1: Immunohistochemistry characteristics in PEACs and MCCs.
(A) The representative Hematoxylin and eosin (H&E) and immunhistochemical staining of PEACs (upper panels) and MCCs (lower panels) were here shown. The neoplastic cells are all cuboidal to tall columnar in hematoxylin and eosin (magnification; ×40, Bar; 500 µm). The immunohistochemical revealed simultaneously staining for CK7, Villin and Ki-67(magnification; ×100, Bar; 200 µm).
(B) Positive staining of ERBB2 by immunohistochemistry in PEAC2, PEAC4, PEAC5 (Score: 3+, 3+, 1+). ERBB2 amplification showing a ERBB2 gene/chromosome 17 ratio >2 as cluster in 80% cells of PEAC2 by FISH (magnification; ×1000).

Table 4: HRD score characteristics of PEACs and MCCs.

	PEAC	MCC	P-value
Total tumor samples(N)	6	16	
Combined HRD scores [a]	32.83±12.50	18.44±5.90	0.001
LOH [a]	8.00±4.00	3.69±1.62	0.001
TAI [a]	11.67±4.89	7.69±2.96	0.029
LST [a]	13.12±5.53	7.06±4.37	0.013
High HRD score (≥ 42) [b]	1/6(16.7%)	0/16(0%)	0.095

HRD: Homologous Recombination Deficiency; LOH: Loss of Heterozygosity; TAI: Telomeric Allelic Imbalance; LST: Large-Scale State Transition. [a]Student t-test, [b]Fisher's exact test for the differences between PEACs and MCCs.

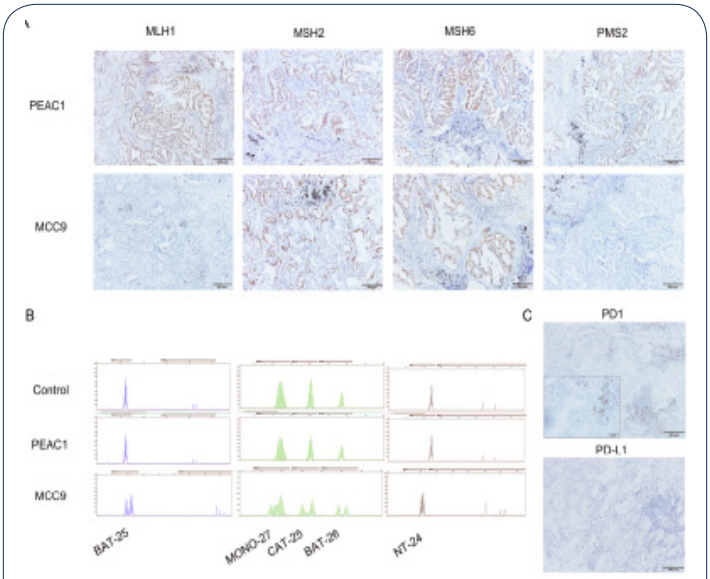

Figure 2: Immune checkpoint blockade analysis of MSI and PD-L1 in PEACs and MCCs.
(A) The representative images of the immunhistochemical markers for mismatch repair in PEAC1 and MCC9 were shown. Nuclear expression of MLH1, MSH2, MSH6 and PMS2 (upper panels). Lack of nuclear expression of MLH1 and PMS2 (lower panels) and was interpreted as being deficient in mismatch repair (magnification; ×100, Bar; 200 µm).
(B) Fragment analysis of PEAC1 for molecular MSI analysis with five markers (CAT-25, MONO-27, NR-24, BAT-25 and BAT-26) within of the Quasi-Monomorphic Variation Range (QMVR). Fragment analysis of MCC9 for molecular MSI analysis in one MSI-H MCC sample with four markers (CAT-25, MONO-27, BAT-25 and BAT-26) outside of the QMVR. Instability is indicated when a peak exceeds the control width. Arrow indicates the allele outside of the QMVR (bp – base pair). Electropherograms show the peak of fluorescein-labeled loci BAT26, NR21, BAT25, MONO27 and NR24.
(C) PD-1 was expressed as positive in interstitial immune cells membrane compartment, but not in tumor cells membrane compartment. Membrane expression of PD-L1 were all-negative in interstitial immune cells and tumor cells membrane compartment.

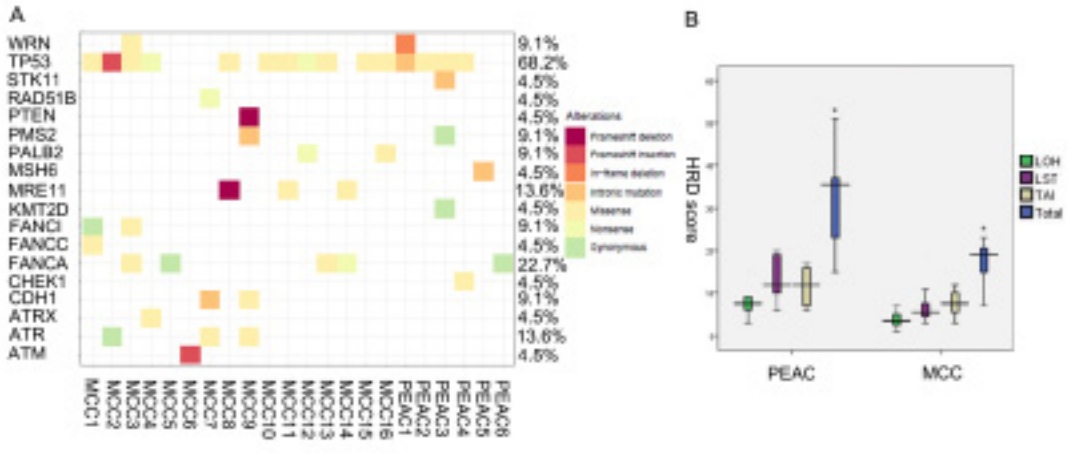

Figure 3: Homologous recombination deficiency characteristics in PEACs and MCCs.
(A) Somatic mutational spectrum of HRD related genes in PEACs and MCCs. Columns represent patients. Rows represent genes. Different types of mutations are denoted in different colors. The frequency of each mutation in this cohort was shown on the right of the oncoprint.
(B) Box plot of HRD scores characteristics. Columns represent scores. Rows represent patients were grouped according to their histopathological diagnosis. Colored boxes indicate different HRD scores (LST, LOH and TAI). *P<0.001.

Discussion

PEAC is a special and rare subtype of pulmonary adenocarcinoma. Up to now, there have been limited less than 30 reports in the English literature. As a primary pulmonary adenocarcinoma, PEAC more or less contains typical pulmonary adenocarcinoma histological components. However, on occasional situations, when the tumor is exclusively composed of glands closely resembling MCC, it is difficult to make a differential diagnosis based solely on their morphologic features. To make a definite diagnosis, the distinctive features of immunohistochemistry and gene mutation profile have been attracting more and more attention. In this context, we investigated the potential differences between PAEDs and MCCs, compared the clinicopathological and molecular characteristics.

Due to its extreme rareness, the molecular signature of PEAC has never been comprehensively explored. In most case reports, the authors focused on the mutational state of several genes involved in lung and colorectal cancer pathogenesis. A recent work by Chen et al. described KRAS as the most commonly mutated gene (48%) and two out of five patients exhibited amplification and/or mutations of ERBB2 in 129 cases of PAED, including 111 from previous literature, but no mutations in EGFR and BRAF were detected [6]. Nottegar et al. identified KRAS mutations in four out of eight PAED samples, with a concomitant PIK3CA gene mutation and EML4-ALK translocation in one case. However, no mutations were detected in EGFR, BRAF and NRAS [9,27]. Zhang et al. applied a larger panel of 259 genes on 13 cases of PAEDs and described the presence of typical NSCLC driver mutations in EGFR, ALK and ERBB2 genes [7]. In line with previous reports, we observed a relatively higher frequency of KRAS mutations in PEAD than other subtypes in pulmonary adenocarcinoma. The mutation frequencies were relatively similar for KRAS in PEACs, compared with MCCs (33.3 versus 37.5%). Meanwhile, we also detected the ERBB2 amplification/mutation in two out of six (33.3%) of PEACs, which were negative in all MCCs. In this regard, the identification of ERBB2 amplification/mutation in PEACs may pave the way to differential diagnosis from MCCs and targeted anti-ERBB2 treatments.

Homologous Recombination Repair (HRR) is a critical pathway for several cellular processes. Deregulated HRR results in genomic instability, which may cause or contribute to carcinogenesis. Importantly, such HRR-defective tumors may be more sensitive to DNA damaging chemotherapeutics such as cisplatin or PARP inhibitors. The altered expression of genes involved in HRR, such as BRCA, PALB2 or FANCD2, had been described in NSCLC [28]. Ding et al. found that 7% of lung adenocarcinomas harbored mutations in the DNA damage response ATM kinase, which was involved in HRR functions [29]. An analysis of 555 adenocarcinoma lung cancer patients from The Cancer Genome Atlas (TCGA) found that 2.5% were carriers of a pathogenic mutation in DNA repair genes (ATM, BRCA2, CHECK2, PARK2, TERT, TP53, YAP1) [30]. Here, the potential deficiency in homologous recombination pathway was found in 50% of PEACs. We reported three PEAC cases with mutations in DNA repair genes, including CHEK1, FANCA, KMT2D, STK11, TP53, WRN.

The genomic scarring in the tumor is permanent, and therefore the HRD score will reflect the tumor's prior HR deficient state. Three HRD scores (TAI, LOH and LST) can be combined to produce a more robust predictor of genomic scarring [20-22]. All three scores were significantly correlated with one another, suggesting that they all measured the same core genomic phenomenon. Marquard et al. evaluated HRD scores in 15 different tumor types, including lung adenocarcinomas. Based on the average of these three scores, lung adenocarcinomas were ranked at 5th position (above colon cancers) [26]. With agreement to above research, we also found the higher score in PEACs than in MCCs. Here, we reported for the first time to presence of high HRD score in PEAC (PEAC6, N=51), suggesting that the patient could benefit from platinum-based chemotherapy and PARP inhibitors. Further study is required to define a robust optimal model for response to clinical agents (platinum-based chemotherapy and PARP inhibitors) in HRD lung cancers, especially in PEACs. In addition to investigate somatic mutations, studying the germline genetic status of PEAC patients and family history are also important for understanding their genetic landscape and for guiding clinical decisions in the future.

Conclusion

In summary, PEAC is an exceptionally rare subtype of invasive lung adenocarcinoma. We shed light on the molecular differences between PEAC and MCC. Our results also underscore, in particular, the relevance of potentially treatable molecular alterations in PEAC, like ERBB2 and HRD. From a clinical view, evaluation of HRD score in PEAC may help to select patients who can benefit from treatments, including platinum compounds and PARP inhibitors.

Declarations

Ethical statement: The authors are accountable for all aspects of the work in ensuring that questions related to the accuracy or integrity of any part of the work are appropriately investigated and resolved. The trial was conducted in accordance with the Declaration of Helsinki (as revised in 2013). Approval was granted by the Ethics Committee on Human Research of the First Affiliated Hospital of Dalian Medical University (Permit number: YJ-KY-FB-2020-27), and written informed consent was obtained from all of the patients before surgery.

Author contributions: All authors contributed to the study conception and design. Investigation and writing-original draft were performed by Lin Zhong. Material preparation and data collection were performed by Chunfang Zhang. Formal analysis and data curation were performed by Wenting Jia. Writing - review and editing were performed by Pengxin Zhang. All authors read and approved the final manuscript.

References

1. Travis WD, Brambilla E, Noguchi M, Nicholson AG, Geisinger KR, et al. International Association for the Study of Lung Cancer/American Thoracic Society/European Respiratory Society international multidisciplinary classification of lung adenocarcinoma. J Thorac Oncol. 2011; 6: 244-285.

2. Tsao MS, Fraser RS. Primary pulmonary adenocarcinoma with enteric differentiation. Cancer. 1991; 68: 1754-1757.

3. Travis WD, Brambilla E, Noguchi M, Nicholson AG, Geisinger K, et al. Diagnosis of lung adenocarcinoma in resected specimens: implications of the 2011 International Association for the Study

of Lung Cancer/American Thoracic Society/European Respiratory Society classification. Arch Patho Lab Med. 2013; 137: 685-705.

4. Wang CX, Liu B, Wang YF, Zhang RS, Yu B, et al. Pulmonary enteric adenocarcinoma: A study of the clinicopathologic and molecular status of nine cases. Int J Clin Exp Pathol. 2014; 7: 1266-1274.

5. Zhao L, Huang S, Liu J, Zhao J, Li Q, et al. Clinicopathological, radiographic, and oncogenic features of primary pulmonary enteric adenocarcinoma in comparison with invasive adenocarcinoma in resection specimens. Medicine (Baltimore). 2017; 96: e8153.

6. Chen M, Liu P, Yan F, Xu S, Jiang Q, et al. Distinctive features of immunostaining and mutational load in primary pulmonary enteric adenocarcinoma: Implications for differential diagnosis and immunotherapy. J Transl Med. 2018; 16: 81.

7. Zhang J, Xiang C, Han Y, Teng H, Li X, et al. Differential diagnosis of pulmonary enteric adenocarcinoma and metastatic colorectal carcinoma with the assistance of next generation sequencing and immunohistochemistry. J Cancer Res Clin Oncol. 2019; 145: 269-279.

8. László T, Lacza A, Tóth D, Molnár TF, Kálmán E. Pulmonary enteric adenocarcinoma indistinguishable morphologically and immunohistologically from metastatic colorectal carcinoma. Histopathology. 2014; 65: 283-287.

9. Nottegar A, Tabbò F, Luchini C, Guerrera F, Gaudiano M, et al. Pulmonary adenocarcinoma with enteric differentiation: Dissecting oncogenic genes alterations with DNA sequencing and FISH analysis. Exp Mol Pathol. 2017; 102: 276-279.

10. Goodman AM, Kato S, Bazhenova L, Patel SP, Frampton GM, et al. Tumor mutational burden as an independent predictor of response to immunotherapy in diverse cancers. Mol Cancer Ther. 2017; 16: 2598-2608.

11. Le DT, Durham JN, Smith KN, Wang H, Bartlett BR, et al. Mismatch-repair deficiency predicts response of solid tumors to PD-1 blockade. Science. 2017; 357: 409-413.

12. Dolled-Filhart M, Roach C, Toland G, Stanforth D, Jansson M, et al. Development of a companion diagnostic for pembrolizumab in non-small cell lung cancer using immunohistochemistry for programmed death ligand-1. Arch Pathol Lab Med. 2016; 140: 1243-1249.

13. Hause RJ, Pritchard CC, Shendure J, Salipante SJ. Classification and characterization of microsatellite instability across 18 cancer types. Nat Med. 2016; 22: 1342-1350.

14. Lin L, Zhuang W, Wang W, Xu C, Chen R, et al. Genetic mutations in lung enteric adenocarcinoma identified using next-generation sequencing. Int J Clin Exp Pathol. 2017; 10: 9583-9590.

15. Jurmeister P, Vollbrecht C, Behnke A, Frost N, Arnold A, et al. Next generation sequencing of lung adenocarcinoma subtypes with intestinal differentiation reveals distinct molecular signatures associated with histomorphology and therapeutic options. Lung Cancer. 2019; 138: 43-51.

16. Vanderstichele A, Busschaert P, Olbrecht S, Lambrechts D, Vergote I. Genomic signatures as predictive biomarkers of homologous recombination deficiency in ovarian cancer. Eur J Cancer. 2017; 86: 5-14.

17. Burrell RA, McClelland SE, Endesfelder D, Groth P, Weller MC, et al. Replication stress links structural and numerical cancer chromosomal instability. Nature. 2013; 494: 492-496.

18. Davies H, Glodzik D, Morganella S, Yates LR, Staaf J, et al. HRDetect is a predictor of BRCA1 and BRCA2 deficiency based on mutational signatures. Nat Med. 2017; 23: 517-525.

19. Lord CJ, Ashworth A. PARP inhibitors synthetic lethality in the clinic. Science. 2017; 355: 1152-1158.

20. Abkevich V, Timms KM, Hennessy BT, Potter J, Carey MS, et al. Patterns of genomic loss of heterozygosity predict homologous recombination repair defects in epithelial ovarian cancer. Br J Cancer. 2012; 107: 1776-1782.

21. Birkbak NF, Wang ZC, Kim J-Y, Eklund AC, Li Q, et al. Telomeric allelic imbalance indicates defective DNA repair and sensitivity to DNA-damaging agents. Cancer Discov. 2012; 2: 366-375.

22. Popova T, Manié E, Rieunier G, Caux-Moncoutier V, Tirapo C, et al. Ploidy and large-scale genomic instability consistently identify basal-like breast carcinomas with BRCA1/2 inactivation. Cancer Res. 2012; 72: 5454-5462.

23. Wolff AC, Hammond ME, Hicks DG, Dowsett M, McShane LM, et al. American Society of Clinical Oncology; College of American Pathologists. Recommendations for human epidermal growth factor receptor 2 testing in breast cancer: American Society of Clinical Oncology/College of American Pathologists clinical practice guideline update. J Clin Oncol. 2013; 31: 3997-4013.

24. Ilie M, Khambata-Ford S, Copie-Bergman C, Huang L, Juco J, et al. Use of the 22C3 anti±PD-L1 antibody to determine PD-L1 expression in multiple automated immunohistochemistry platforms. PLoS One. 2017; 12: e0186537.

25. Richards S, Aziz N, Bale S, Bick D, Das S, et al. ACMG Laboratory Quality Assurance Committee. Standards and guidelines for the interpretation of sequence variants: A joint consensus recommendation of the American College of Medical Genetics and Genomics and the Association for Molecular Pathology. Genet Med. 2015; 17: 405-424.

26. Marquard AM, Eklund AC, Joshi T, Krzystanek M, Favero F, et al. Pan-cancer analysis of genomic scar signatures associated with homologous recombination deficiency suggests novel indications for existing cancer drugs. Biomark Res. 2015; 3: 9.

27. Nottegar A, Tabbò F, Luchini C, Brunelli M, Bria E, et al. Pulmonary adenocarcinoma with enteric differentiation: immunohistochemistry and molecular morphology. Appl Immunohistochem Mol Morphol. 2018; 26: 383-387.

28. Kadouri L, Rottenberg Y, Zick A, Hamburger T, Lipson D, et al. Homologous recombination in lung cancer, germline and somatic mutations, clinical and phenotype characterization. Lung Cancer. 2019; 137: 48-51.

29. Ding L, Getz G, Wheeler DA, Mardis ER, McLellan MD, et al. Somatic mutations affect key pathways in lung adenocarcinoma. Nature. 2008; 455: 1069-1075.

30. Parry EM, Gable DL, Stanley SE, Khalil SE, Antonescu V, et al. Germline mutations in DNA repair genes in lung adenocarcinoma. J Thorac Oncol. 2017; 12: 1673-1678.